

Dipole Equilibrium and Stability

J. Kesner³, A.N. Simakov³, D.T. Garnier¹, P.J. Catto², R.J. Hastie³,
S.I. Krasheninnikov⁴, M.E. Mauel¹, T. Sunn Pedersen¹, J.J. Ramos³

1) Columbia University, New York, NY

2) MIT, Cambridge, MA and Lodestar Research Corporation, Cambridge, MA, USA.

3) MIT, Cambridge, MA

4) University of California, San Diego, CA

Abstract. A plasma confined in a dipole field exhibits unique equilibrium and stability properties. In particular, equilibria exist at all β values and these equilibria are found to be stable to ballooning modes when they are interchange stable. When a kinetic treatment is performed at low beta we also find a drift temperature gradient mode which couples to the MHD mode in the vicinity of marginal interchange stability.

1 Introduction

A dipole plasma confinement device may be an attractive fusion power source [1, 2] since it can be stable to MHD instabilities when the pressure and density gradients are sufficiently gentle. The relatively rapid radial variation of the magnetic field strength allows very high plasma pressure near the levitated dipole coil while maintaining a much lower plasma pressure at the outer edge. A critical issue for the dipole fusion concept is the nature of plasma equilibrium and stability at very high core plasma pressure and local plasma beta. In this paper, we present models of high beta equilibria that indicate that plasmas can be MHD stable in a dipole magnetic field even when the local beta greatly exceeds unity.

Dipole MHD equilibrium and stability have been analyzed both analytically and numerically [3, 4, 5]. The stability of numerically computed free boundary equilibria for a plasma in the field of a floating ring provides realistic targets that appear achievable and will provide a test of dipole equilibrium and stability [3]. A useful family of equilibrium solutions to the Grad-Shafranov equation has been found for a point dipole by semi-analytic methods [4]. The MHD stability problem could then be reduced to a problem of solving a linear ordinary integro-differential equation [5]. The point dipole equilibria utilizes a sub-critical pressure profile that is always interchange stable. These point dipole solutions are valid for arbitrary plasma pressure. Both the numerical floating ring equilibria and the point dipole equilibria for isotropic plasma pressure have been found to remain stable to ballooning modes at all beta values when they are interchange stable.

Electrostatic plasma modes for magnetic dipole equilibria (the limit of low plasma pressure) have also been studied kinetically [6] under the high collisionality assumption. These modes are flute-like to leading order in the expansion in $(k_{\perp}\rho_i)^2 \ll 1$, where ρ_i is the ion Larmor radius and k_{\perp} is the perpendicular component of a perturbation wave vector. The electrostatic modes dispersion relation appears to have two branches - an

$\omega \gg \omega_*, \omega_d$ “MHD-like” branch and an $\omega \sim \omega_*, \omega_d$ “drift” branch, where ω , ω_* and ω_d are the mode, diamagnetic drift and magnetic drift frequencies. In the absence of collisional dissipation the stability condition of the “MHD-like” electrostatic mode coincides with the MHD interchange stability condition, while stability of the “drift” mode depends on two independent parameters: $\eta \equiv d \ln T_i / d \ln N_i$ and $d \equiv -d \ln p / d \ln \nu$, where T_i and N_i are the ion temperature and density, p is the plasma pressure and $\nu = \oint d\ell / B$ with B the magnitude of the magnetic field and ℓ the coordinate along the magnetic field line.

In the Levitated Dipole Experiment (LDX) [7] now under construction, the dipole magnetic field will be created by a floating axisymmetric superconducting current ring (there is no toroidal magnetic field). The device is designed to explore the confinement and stability of a high- β plasma confined in a dipole magnetic field. Figure 1 displays the vacuum field of the device when the floating coil is charged. The floating coil is maintained at the midplane of the vacuum vessel by attraction to a coil located above the vacuum chamber and an x-point is evident due to cancellation of fields near the upper wall of the vacuum chamber. Feedback control is required to maintain vertical stability of the ring. Shaping coils form an outside separatrix and will permit studies of plasma equilibrium and stability as the magnetic configuration changes.

2 Ideal MHD Formulation

2.1 Equilibrium

In a laboratory plasma confined in a levitated dipole device the plasma is expected to be isotropic. Since the currents in the floating ring are toroidal, the magnetic field is entirely poloidal and currents within the plasma are toroidal as well. All magnetic field lines are closed so that “flux” or pressure surfaces are determined by their surfaces of rotation about the symmetry axis. The Grad-Shafranov equation for a dipole is particularly simple in form:

$$\nabla \cdot \left(\frac{\nabla \psi}{R^2} \right) = -\mu_0 \frac{dp}{d\psi}, \quad (1)$$

with ψ the poloidal flux function, $\mathbf{B} = \nabla \psi \times \mathbf{e}_\zeta / R$, and R, Z, ζ cylindrical coordinates. The plasma pressure is a flux function, i.e. $p = p(\psi)$. We will define the local beta as $\beta = 2\mu_0 p / B^2$ and represent the beta value on the outer midplane at the location of the magnetic field minimum ($Z=0, R > R_{ring}$) as β_0 .

2.1.1 High β Equilibrium in LDX: Numerical Solution

We have solved the equilibrium equation numerically for LDX (at arbitrary beta) [3]. The code uses a multi-grid relaxation method to find a free boundary solution to Eq. (1) by iteratively updating the grid boundary conditions and solving the appropriate fixed boundary problem at each iteration [8, 9].

For a fixed edge pressure the highest beta value is obtained for a pressure profile that is marginally stable to interchange modes. We have found that MHD ballooning modes remain stable at high beta values and therefore we can assume a relatively high edge beta ($\beta_{edge} = \beta_0(R = R_{wall})$). This does not imply a high edge pressure since the magnetic field of a dipole falls off as R^{-3} and it will be low (60 G in LDX) at the outer vacuum chamber wall. At marginal stability, for a dipole, pressure will fall rapidly moving towards the wall ($p \propto \nu^{-\gamma}$, $\gamma = 5/3$) although beta falls more slowly ($\beta \propto 1/(B^2 \nu^\gamma) \sim 1/(L^\gamma B^{1/3})$, $L = B \oint d\ell/B$). A high- β equilibrium solution, shown in Fig. 2, is found by choosing a pressure profile that is close to the interchange stability boundary ($p \propto \nu^{-\gamma}$ [10]) and has an edge pressure of 20 Pa which yields $\beta_{edge} = 0.67$. The corresponding peak beta is $\beta_{max} = 25$ at $R = 0.85 m$ and the plasma has effectively excluded the field in this region. Notice that the equilibrium has shifted outward radially and the plasma is now limited on an outer limiter and not on the magnetic separatrix.

2.1.2 Point Dipole Equilibrium: Semi-Analytical Solution

For a point dipole it is possible to obtain relatively simple separable solutions of the Grad-Shafranov equation for both the isotropic [4] and anisotropic [11] pressure cases.

For isotropic pressure we look for a solution of Eq. (1) in a form [4] $\psi = \psi_0 (R_0/r)^\alpha h(\mu)$, where $\mu = \cos \theta$, θ is a poloidal angle, h is an unknown function of μ only, α is an unknown eigenvalue ($0 < \alpha < 1$), and R_0 is a cylindrical radius at which the surface ψ_0 intersects the symmetry plane $\mu = 0$. In order for h to be a function of μ only we must assume $p = p_0 (\psi/\psi_0)^{2+4/\alpha}$. Then $\beta = \beta(\mu)$ and $\beta_0 = \beta(\mu = 0)$. In this case Eq. (1) can be transformed into a nonlinear second order differential equation for h

$$\frac{d}{d\mu} \left[(1 - \mu^2)^2 \frac{d}{d\mu} \left(\frac{h}{1 - \mu^2} \right) \right] - (1 - \alpha)(2 + \alpha)h = -\beta_0 \alpha (2 + \alpha) (1 - \mu^2) h^{1+4/\alpha} \quad (2)$$

with boundary conditions $h(|\mu| \rightarrow 1) \rightarrow (1 - |\mu|)$ and $dh/d\mu|_{\mu=0} = 0$.

Equation (2) must then in general be solved numerically but the limiting cases of large and small β_0 are found analytically to give $1 - \alpha = (512/1001) \beta_0$ for $\beta_0 \ll 1$ and $\alpha = 1/\beta_0^{1/2}$ for $\beta_0 \gg 1$. Notice that the separable solution of the Grad-Shafranov equation exists for arbitrarily large β_0 . The dependence of $\alpha(\beta_0)$ can be found numerically and is shown in Fig. 3. As β_0 increases the constant ψ surfaces become more and more extended and localized about the symmetry plane, resembling an accretion disk, as shown in Fig. 4, where the magnetic field lines are shown for $\beta = 0$ (the vacuum case) and $\beta = 20$.

In the presence of pressure anisotropy the Grad-Shafranov equation can be written as [12]

$$\nabla \cdot \left[\frac{\nabla \psi}{R^2} \left(1 + \frac{p_\perp - p_\parallel}{B^2/\mu_0} \right) \right] = -\mu_0 \frac{\partial p_\parallel}{\partial \psi}, \quad (3)$$

where p_{\parallel} and p_{\perp} are functions of ψ and B and the ψ derivative in Eq. (3) is performed at fixed B . In Ref. [11] a separable solution of Eq. (3) is found for $p_{\perp} = (1 + 2a)p_{\parallel}$, where $a > -1/2$ is an adjustable constant anisotropy parameter. Then $p_{\parallel} = p(\psi)(B_0/B)^a$, where $B_0 = \alpha\psi_0/R_0^2$ is a constant, $p(\psi) = p_0(\psi/\psi_0)^{2(1+a)(2+\alpha)/\alpha}$, and Eq. (3) can be rewritten as a nonlinear second order differential equation for $h(\mu)$ with the eigenvalue α .

It is well known that, unlike the isotropic pressure case, the anisotropic pressure equilibrium does not exist for arbitrarily large β_0 , because it is destroyed by either a fire hose instability for $p_{\parallel} > p_{\perp}$ ($a < 0$) or a mirror mode instability for $p_{\perp} > p_{\parallel}$ ($a > 0$). In particular, for the equilibrium of Ref. [11], $\beta_0 < \beta_{mm} \equiv (1 + a) / [a(1 + 2a)]$ for $a > 0$, and $\beta_0 < \beta_{fh} \equiv -(1 + a) / a$ for $a < 0$.

As in the isotropic pressure case, the equation for h must be solved numerically, but it can be shown analytically that for $\beta_0 \gg 1$, $\alpha \approx 1/\beta_0^{1/2}$ as before.

2.2 Ideal MHD Stability

2.2.1 Energy Principle and Interchange Stability for Isotropic Pressure

The ideal MHD interchange and ballooning stability of the magnetic dipole configuration can be evaluated using the MHD energy principle. We will employ the notation of Ref. [13]. For a levitated dipole the magnetic field is purely poloidal, field lines are closed and the curvature is in the $\nabla\psi$ direction, i.e. $\boldsymbol{\kappa} = \kappa_{\psi}\nabla\psi$ with $\boldsymbol{\kappa} = \mathbf{b} \cdot \nabla\mathbf{b}$ and $\mathbf{b} \equiv \mathbf{B}/B$. Due to the absence of parallel currents the kink driving term is zero for a dipole. Minimizing the potential energy $\delta W_F \propto \omega^2$ with respect to the parallel plasma displacement results in an expression for δW_F with a stabilizing plasma compressibility term due to closed field lines:

$$\delta W_F = \frac{1}{2\mu_0} \int_p d^3r \left[Q_{\perp}^2 + B^2(\nabla \cdot \boldsymbol{\xi}_{\perp} + 2\boldsymbol{\xi}_{\perp} \cdot \boldsymbol{\kappa})^2 + \gamma\mu_0 p \langle \nabla \cdot \boldsymbol{\xi}_{\perp} \rangle_{\theta}^2 - 2\mu_0(\boldsymbol{\xi}_{\perp} \cdot \nabla p)(\boldsymbol{\kappa} \cdot \boldsymbol{\xi}_{\perp}) \right], \quad (4)$$

where $\mathbf{Q} = \nabla \times (\boldsymbol{\xi}_{\perp} \times \mathbf{B})$, $\boldsymbol{\xi}_{\perp}$ is the perpendicular plasma displacement and the field line average is defined as $\langle \dots \rangle_{\theta} = \nu^{-1} \oint (\dots) d\ell / B$, with $\nu = \oint d\ell / B$.

The first term in Eq. (4) represents the energy associated with field line bending, and the second and the third terms are due to the stabilizing influence of magnetic field line compression and plasma compression, respectively. The plasma compression term appears only for a closed field lines system. The last term is the curvature (instability) drive.

Writing the perpendicular displacement as

$$\boldsymbol{\xi}_{\perp} = \left(\xi / R^2 B^2 \right) \nabla\psi - \eta R^2 \nabla\zeta,$$

we can minimize Eq. (4) with respect to η . Noticing that the modes with highest toroidal

numbers n are the most unstable we consider $n \rightarrow \infty$ limit (see Refs. [5, 10] for details). Then minimization of δW_F for $n \rightarrow \infty$ gives

$$B^2 (\nabla \cdot \boldsymbol{\xi}_\perp + 2\boldsymbol{\kappa} \cdot \boldsymbol{\xi}_\perp) + \mu_0 \gamma p \langle \nabla \cdot \boldsymbol{\xi}_\perp \rangle_\theta = 0,$$

which also implies $\eta \rightarrow 0$ as $\partial/\partial\zeta \propto n$. Using the preceding equation to eliminate $\nabla \cdot \boldsymbol{\xi}_\perp$ and $\langle \nabla \cdot \boldsymbol{\xi}_\perp \rangle_\theta$ from Eq. (4) we obtain the reduced energy principle

$$\delta W_F = \frac{1}{2\mu_0} \int_p d^3r \left[Q_\perp^2 + \frac{4\mu_0 \gamma p \langle \boldsymbol{\kappa} \cdot \boldsymbol{\xi}_\perp \rangle_\theta^2}{1 + \mu_0 \gamma p \langle B^{-2} \rangle_\theta} - 2\mu_0 (\boldsymbol{\xi}_\perp \cdot \nabla p) (\boldsymbol{\kappa} \cdot \boldsymbol{\xi}_\perp) \right], \quad (5)$$

where now $\boldsymbol{\xi}_\perp = (\xi/R^2 B^2) \nabla \psi$ and $Q_\perp^2 = R^{-2} B^{-2} (\mathbf{B} \cdot \nabla \xi)^2$.

Considering interchange modes, for which $\mathbf{B} \cdot \nabla \xi = 0$ (i.e. $Q_\perp^2 = 0$), we obtain from Eq. (5) the general finite β interchange stability condition

$$2\gamma p \langle \boldsymbol{\kappa} \cdot \nabla \psi / R^2 B^2 \rangle_\theta > \left(1 + \mu_0 \gamma p \langle B^{-2} \rangle_\theta \right) (dp/d\psi), \quad (6)$$

which can be rewritten [4, 5] as

$$\frac{1}{p} \frac{dp}{d\psi} + \frac{\gamma}{\nu} \frac{d\nu}{d\psi} < 0. \quad (7)$$

2.2.2 Ballooning Stability for Isotropic Pressure

We next consider the ballooning stability of a magnetic dipole configuration. We notice here that short-wavelength ballooning modes bend magnetic field lines, which, along with plasma compression, has a stabilizing influence on the modes. Introducing the perpendicular plasma kinetic energy

$$K = \frac{1}{2} \int_p d^3r \rho \xi_\perp^2, \quad (8)$$

as the normalization, with $\boldsymbol{\xi}_\perp$ the perpendicular plasma displacement, we can minimize the functional

$$\Lambda = \frac{\delta W_F}{K} \propto \omega^2,$$

where δW_F is given by Eq. (5) (with $Q_\perp^2 \neq 0$). Varying with respect to ξ to obtain the infinite n integro-differential ballooning equation gives

$$B \frac{d}{d\ell} \left(\frac{1}{BR^2} \frac{d\xi}{d\ell} \right) + \mu_0 \left(2\kappa_\psi \frac{dp}{d\psi} + \Lambda \frac{\rho}{R^2 B^2} \right) \xi = 4\mu_0 \gamma p \kappa_\psi \frac{\langle \kappa_\psi \xi \rangle_\theta}{1 + \gamma \langle \beta \rangle_\theta}. \quad (9)$$

As is shown in Ref. [10], some key properties of the eigenvalues Λ_j , $j = 0, 1, 2, \dots$, of Eq. (9) can be determined based on the eigenvalues λ_j of the corresponding Sturm-Liouville differential equation

$$B \frac{d}{d\ell} \left(\frac{1}{BR^2} \frac{d\xi}{d\ell} \right) + \mu_0 \left(2\kappa_\psi \frac{dp}{d\psi} + \lambda \frac{\rho}{R^2 B^2} \right) \xi = 0, \quad (10)$$

which has a complete set of eigenfunctions ξ_j with corresponding distinct eigenvalues λ_j , that can be arranged as an increasing set for specified boundary conditions. As the dipole system is up-down symmetric, the eigenfunctions of Eq. (10) are up-down symmetric or antisymmetric, and we assign even (odd) indices j to the symmetric (antisymmetric) eigenfunctions and eigenvalues in such a way that the smaller index corresponds to the eigenfunction with a smaller eigenvalue. Notice that in general the eigenvalues for the even and odd eigenfunctions form two independent increasing sets as the corresponding boundary conditions are different. As is shown in Ref. [10] $\lambda_{2j+1} = \Lambda_{2j+1} \leq \lambda_{2j+3} = \Lambda_{2j+3}$ and $\lambda_{2j} \leq \Lambda_{2j} \leq \lambda_{2j+2} \leq \Lambda_{2j+2}$. As a result, $\lambda_0 \geq 0$ and $\lambda_1 \geq 0$ lead to $\Lambda_j \geq 0$ and ballooning stability, while $\lambda_1 \leq 0$ or $\lambda_2 \leq 0$ lead to $\Lambda_1 \leq 0$ or $\Lambda_0 \leq 0$ and ballooning instability. For the more subtle case $\lambda_0 < 0 < \lambda_2$ and $\lambda_1 = \Lambda_1 > 0$ it is shown in Ref. [10] that the equilibrium is ballooning stable and $\Lambda_0 > 0$ (unstable and $\Lambda_0 < 0$), if it is interchange stable (unstable). Further details of this analysis are given in Ref. [5].

2.2.3 MHD Stability of the Point Dipole Equilibrium and of a High Beta Equilibrium in a Field of a Levitated Dipole for Isotropic Pressure

For the point dipole equilibrium of Ref. [4] $p \propto \psi^{2+4/\alpha}$ and $\nu \propto \psi^{-1-3/\alpha}$, so that Eq. (7) can be rewritten as $\gamma > 2(2 + \alpha) / (3 + \alpha) > 4/3$ for $0 < \alpha < 1$, which is always true, so the point dipole equilibrium is always interchange stable.

Ballooning stability of this equilibrium was studied in Ref. [5]. Eigenvalues of Eq. (10) were obtained both analytically in the limiting cases of large and small β_0 and numerically for arbitrary β_0 . It was found that $\lambda_0 < 0$ and $\lambda_2 > \lambda_1 > 0$, so that the point dipole equilibrium is always ballooning stable because it is interchange stable.

Reference [3] studied interchange and ballooning stability of a laboratory plasma confined in the field of a circular floating coil. It was found that a high beta MHD equilibrium with a peak local beta of $\beta \sim 10$ and volume averaged beta of $\bar{\beta} \sim 0.5$, obtained numerically, with a pressure profile near marginal stability for interchange modes, is ballooning stable for the first antisymmetric ballooning mode of Eq. (10). Since the lowest symmetric ballooning mode and the interchange mode are identical at marginality [5], LDX would be MHD stable for such equilibria.

2.2.4 Anisotropic Pressure MHD Stability

When radio frequency heating is used to increase the plasma temperature a mild pressure anisotropy may result. Stronger anisotropies are of interest for space and astrophysical dipole configurations where the dipole field is generated by a dynamo mechanism. Consequently, the interchange and ballooning stability of an anisotropic pressure plasma confined by a dipole magnetic field has also been investigated.

An anisotropic fluid energy principle (which reduces to the isotropic limit) has been derived in Ref. [14] from the Kruskal-Oberman [15, 16] formulation in which the plasma is treated kinetically along the magnetic field and as a fluid across the magnetic field. Anisotropic forms of the interchange stability criterion and of the ballooning mode equation, including plasma compressibility, have been obtained. This stability analysis has been applied to the anisotropic pressure family of point dipole equilibria [11]. As was mentioned earlier the mirror instability or firehose instability set limits on the achievable plasma beta, β_0 , when the perpendicular pressure p_\perp is greater (mirror) or less than (firehose) the parallel pressure p_\parallel . In Ref. [14] it was found that the point dipole equilibria of Ref. [11] are interchange stable for all plasma betas up to the β_{mm} or β_{fh} , whichever is appropriate. At the same time ballooning modes are stable for all betas up to some critical value, which is below β_{mm} for $1 < p_\perp/p_\parallel < 8$ and is equal to β_{mm} for $p_\perp/p_\parallel > 8$. At modest anisotropy the beta threshold may be observable in the high beta plasmas expected in LDX (for $p_\perp/p_\parallel = 1.2$ the beta limit becomes $\beta_{limit} \approx 6$).

2.3 Low- β Collisional Interchange Modes

We have shown that MHD predicts that at low beta interchange modes limit the pressure gradients that can be stably maintained. Ideal MHD assumes a particularly simple equation of state and ignores finite Larmor radius effects which can become important for ions. We would expect a more detailed kinetic stability treatment to produce drift waves as well as MHD “fluid” modes. We can shed light on these assumptions by considering the stability of electrostatic interchange modes in a collisional plasma [6].

To compare the MHD results with those of kinetic theory we define

$$\omega_{*pi} \equiv \frac{ncT_i}{Z_i e} \frac{1}{p} \frac{dp}{d\psi} \quad (11)$$

and

$$\omega_{di} \equiv \frac{ncT_i}{Z_i e R B} \mathbf{e}_\zeta \cdot \mathbf{b} \times (\nabla \ln B + \boldsymbol{\kappa}), \quad (12)$$

and find that

$$\langle \omega_{di} \rangle_\theta = -\frac{ncT_i}{Z_i e \nu} \frac{d\nu}{d\psi}, \quad (13)$$

where c is the speed of light, $T_i = T_i(\psi)$ and $Z_i e$ are the ion temperature and charge, $\nu = \oint d\ell/B$ and $n \gg 1$ is the toroidal mode number. At low β the MHD stability condition (the interchange stability condition, given by Eq. (7)) can then be written as $\omega_{*pi} < \gamma \langle \omega_{di} \rangle_\theta$ or

$$d < \frac{5}{3}, \quad (14)$$

where $d = -d \ln p / d \ln \nu$.

We then solve the Boltzmann equation in the high collision frequency limit for both ions and electrons and therefore apply the following orderings:

$$\Omega \gg \omega_b \gg \nu_c \gg \omega_* \sim \omega_d \sim \omega, \quad (15)$$

with Ω the cyclotron frequency, ω_b the bounce frequency, ν_c the collision frequency, ω_* the diamagnetic drift frequency, and ω_d the magnetic curvature drift frequency.

Following the treatment of Ref. [17], modified to account for collisions [18], it can be shown that within the eikonal approximation the perturbed distribution function f_j , $j = i, e$, is given by [18]

$$f_j = \left(-\frac{Z_j e}{T_j} \hat{\Phi}_1 f_{Mj} + h_j e^{iL_j} \right) e^{iS - i\omega t}, \quad (16)$$

where h_j is a solution of the following equation

$$v_{\parallel} \mathbf{b} \cdot \nabla h_j - i(\omega - \tilde{\omega}_{dj}) h_j = \left\langle e^{-iL_j} C_j \left(h_j e^{iL_j} \right) \right\rangle_{\phi} + \hat{Q} J_0 \left(\frac{k_{\perp} v_{\perp}}{\Omega_j} \right). \quad (17)$$

Here we assume that the perturbed potential $\Phi_1 = \hat{\Phi}_1 e^{iS - i\omega t}$, where S is the eikonal, $L_j \equiv (\mathbf{v} \cdot \mathbf{b} \times \mathbf{k}_{\perp}) / \Omega_j$ and $\mathbf{k}_{\perp} \equiv \nabla S$. In the above expressions

$$f_{Mj}(E, \psi) = N_j(\psi) (M_j / 2\pi T_j(\psi))^{3/2} e^{-M_j E / T_j(\psi)}$$

$$\hat{Q} = -i \frac{Z_j e}{T_j} f_{Mj} \hat{\Phi}_1 \left\{ \omega - \omega_{*j} \left[1 + \eta_j \left(\frac{M_j E}{T_j} - \frac{3}{2} \right) \right] \right\}$$

with the energy E given by $E = v^2/2$, $\eta_j = d \ln T_j / d \ln N_j$, J_0 is a Bessel function, M_j , Ω_j and C_j are the mass, cyclotron frequency and linearized collision operator for species j , ϕ is a gyrophase and $\langle \dots \rangle_{\phi} = \oint d\phi (\dots) / 2\pi$. We also introduced

$$\tilde{\omega}_{dj} = \mathbf{k}_{\perp} \cdot \mathbf{b} \times \left(\frac{v_{\perp}^2}{2\Omega_j} \nabla \ln B + \frac{v_{\parallel}^2}{\Omega_j} \mathbf{b} \cdot \nabla \mathbf{b} \right),$$

$$\omega_{*j} = \frac{ncT_j}{Z_j e N_j} \frac{dN_j}{d\psi},$$

and assumed that the equilibrium electric potential $\Phi_0 = 0$. Notice that h_j in Eq. (17) is independent of the gyrophase.

Suppressing the index j for simplicity, expanding $h = h^0 + h^1 + h^2 + \dots$, and assuming $|L| \ll 1$, Eq. (17) gives to leading order

$$v_{\parallel} \mathbf{b} \cdot \nabla h^0 = \left\langle C(h^0) \right\rangle_{\phi} - i \left\langle LC(h^0) \right\rangle_{\phi} + i \left\langle C(Lh^0) \right\rangle_{\phi}, \quad (18)$$

so that

$$h^0 = f_M(E, \psi) \left(\alpha(\psi) + \beta(\psi) \frac{v^2}{2} \right). \quad (19)$$

To the next order Eq. (17) gives

$$-(\omega - \tilde{\omega}_d) h^0 + v_{\parallel} \mathbf{b} \cdot \nabla h^1 = \langle C(h^1) \rangle_{\phi} + \langle LC(Lh^0) \rangle_{\phi} - \langle C(L^2 h^0/2) \rangle_{\phi} + \hat{Q} J_0 \left(\frac{k_{\perp} v_{\perp}}{\Omega_j} \right). \quad (20)$$

Integrating Eq. (20) over d^3v with a weighting function v^q with $q = 0$ and 2 , and then field line (or poloidal angle) averaging the resulting expression annihilates the second term on the left hand side and the first and the third terms on the right hand side. The result is two linear algebraic equations for the $\alpha(\psi)$ and $\beta(\psi)$ defined in Eq. (19):

$$\left\langle \int d^3v v^q (\omega - \tilde{\omega}_d) h^0 \right\rangle_{\theta} = i \left\langle \int d^3v v^q \hat{Q} J_0 \left(\frac{k_{\perp} v_{\perp}}{\Omega} \right) \right\rangle_{\theta}, \quad (21)$$

where finite Larmor radius effects must be retained for ions only, and collisional modifications to the right hand side have been neglected. The finite collisional dissipation effects, which come from the collisional term neglected in (21), and are proportional to $\nu_{ii} \bar{b}$, where ν_{ii} is the ion-ion collision frequency and $\bar{b} \equiv \langle b_i \rangle_{\theta} = \langle k_{\perp}^2 T_i / M_i \Omega_i^2 \rangle_{\theta}$, can be important and can significantly change the stability of the electrostatic modes [19].

We can perform integration and averaging in Eq. (21), solve the resulting equations for α and β , and then form h_0 , f_e and f_i using Eqs. (19) and (16). We then evaluate the perturbed electron and ion densities $N_j = \int d^3v f_j$ and obtain the dispersion relation using the quasi-neutrality condition. It can be shown that the electrostatic modes are flute-like (up-down symmetric) to leading order in the expansion in b_i . Using this fact to simplify the dispersion relation and introducing the dimensionless parameters $\lambda = \omega / \langle \omega_{di} \rangle_{\theta}$, $d = \omega_{*i} (1 + \eta_i) / \langle \omega_{di} \rangle_{\theta} = -d \ln p / d \ln \nu$, and $\eta \equiv \eta_i$ we eventually find [6]

$$\left(d - \frac{5}{3} \right) \lambda^2 + \frac{5}{9} \left(d \frac{3\eta - 7}{1 + \eta} + 5 \right) + \left(\frac{\bar{b}}{2} \right) \left[\lambda^4 - \left(d - \frac{5}{3} \right) \lambda^3 - \frac{5}{9} \left(3d \frac{1 + 2\eta}{1 + \eta} + 7 \right) \lambda^2 - \frac{5}{9} \left(d \frac{3\eta - 7}{1 + \eta} + 5 \right) \lambda + \frac{25}{9} \frac{d}{1 + \eta} \right] = 0, \quad (22)$$

where we have assumed $Z_i T_i = T_e$.

This equation appears to have two classes of solutions - high-frequency or “MHD-like” modes for which $\lambda \gg 1$ and low-frequency or “drift temperature gradient” (or DTG) modes for which $\lambda \sim 1$. The modes are uncoupled for $\bar{b}^{1/2} \ll |d - 5/3|$. The “MHD-like” mode is obtained when the first term of the dispersion relation (22) is balanced by the third one, so that we find

$$\left(\frac{\omega}{\langle \omega_{di} \rangle_{\theta}} \right)_{MHD} = \pm \left[\frac{2(5/3 - d)}{\bar{b}} \right]^{1/2}. \quad (23)$$

This mode is stable (unstable) when $d < 5/3$ ($d > 5/3$), as found earlier from ideal MHD. However, collisional modifications of order ω_d/ν_{ii} that arise from next order corrections to h in the bounce frequency expansion (15) may result in terms which are more important than the finite \bar{b} terms in Eq. (22). These collisional terms differ from the classical cross field transport terms ($\propto \nu_{ii}\bar{b}$) mentioned below Eq. (21) [19]. They arise from the collisional relaxation of an anisotropic $h(E, \mu)$ towards a Maxwellian, as discussed in Ref. [20] for a straight magnetic geometry.

To consider the DTG modes we neglect the finite Larmor radius terms proportional to \bar{b} in the dispersion relation, and obtain

$$\left(\frac{\omega}{\langle\omega_{di}\rangle_\theta}\right)_{DTG} = \pm \sqrt{\frac{5}{9} \frac{5 - d^{\frac{7-3\eta}{1+\eta}}}{\frac{5}{3} - d}}. \quad (24)$$

The stability and instability regions of the DTG modes are shown in Fig. 5 in white and grey, respectively. Notice that for $d < 5/3$ (the MHD stable regime) there are regions where the DTG mode is unstable. In particular, near the MHD stability boundary $d = 5/3$ instability occurs for $-1 < \eta < 2/3$. Negative d corresponds to the regions near the ring.

The two collisional modifications mentioned in the preceding paragraphs are currently under investigation and are expected to modify the high frequency “MHD-like” mode of Eq. (23) and alter the stability of the low frequency DTG mode of Eq. (24).

3 Acknowledgements

This work was supported by the U.S. Department of Energy.

References

- [1] Hasegawa, A., Comments Plasma Phys. Control. Fusion **1** (1987) 147.
- [2] Hasegawa, A., Chen, L., Mauel, M., Nucl. Fusion **30** (1990) 2405.
- [3] Garnier, D.T., Kesner, J., Mauel, M.E., Phys. Plasmas **6** (1999) 3431.
- [4] Krasheninnikov, S.I., Catto, P.J., Hazeltine, R.D., Phys. Rev. Lett. **82** (1999) 2689.
- [5] Simakov, A.N., Catto, P.J., Krasheninnikov S.I., Ramos, J.J., Phys. Plasmas **7** (2000) 2526.
- [6] Kesner, J., Phys. Plasmas **7** (2000) 3837.
- [7] Kesner, J., Bromberg, L., Garnier, D.T., Mauel, M.E., *Fusion Energy 1998* (International Atomic Energy Agency, Vienna, 1999) vol.3 p. 1165.
- [8] Interpretive equilibrium code written for tokamak geometry was obtained from Mauel, M.
- [9] Lao, L.L., StJohn, H., Stambaugh, R.D. et al., Nucl. Fusion **25** (1985) 1611.
- [10] Bernstein, I.B., Frieman, E.A., Kruskal, M.D., Kulsrud, R.M., Proc. R. Soc. London, Ser. A **244** (1958) 17.
- [11] Krasheninnikov S.I., Catto, P.J., Phys. Plasmas **7** (2000) 626.
- [12] Mercier, C., Cotsaftis, M., Nucl. Fusion **1** (1961) 121.

- [13] J.P. Freidberg, *Ideal Magnetohydrodynamics* (Plenum, New York, 1987).
- [14] Simakov, A.N., Hastie, R.J., Catto, P.J., Phys. Plasmas **7** (2000) 3309.
- [15] Kruskal, M., Oberman, C., Phys. Fluids **1** (1958) 275
- [16] Taylor, J.B., Hastie R.J., Phys. Fluids **8** (1965) 323.
- [17] Tang, W.M., Connor, J.W., Hastie, R.J., Nucl. Fusion **20** (1980) 1439.
- [18] Connor, J.W., Chen, L., Phys. Fluids **28** (1985) 2201.
- [19] A. B. Mikhailovskii, *Electromagnetic Instabilities in an Inhomogeneous Plasma* (IOP Publishing, London, 1992).
- [20] Mikhailovskii, A. B., Tsypin, V.S., Sov. Phys.-JETP **32** (1971) 287.

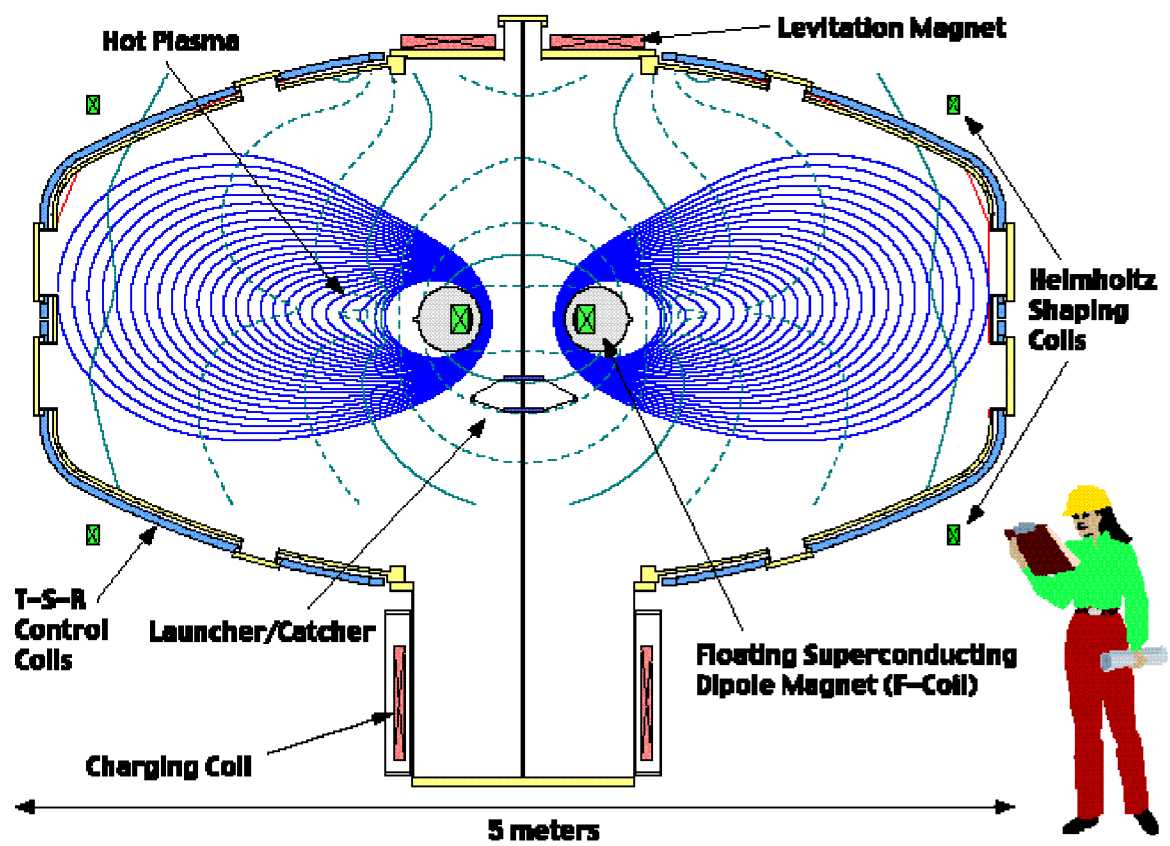


Figure 1: The Levitated Dipole Experiment.

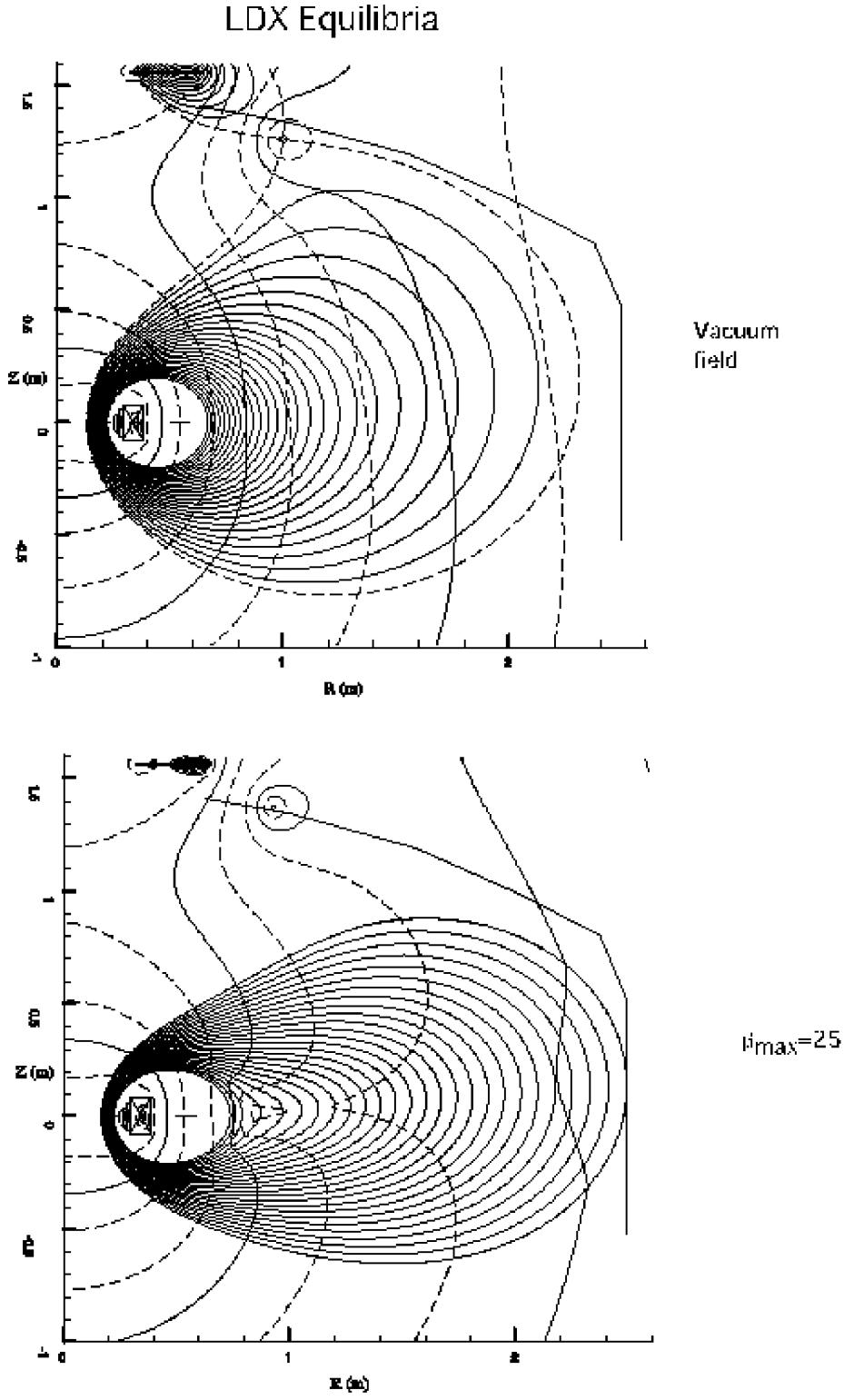


Figure 2: Low (vacuum field) and high β equilibrium ($\beta_{\max} = 25$) solution in the LDX geometry.

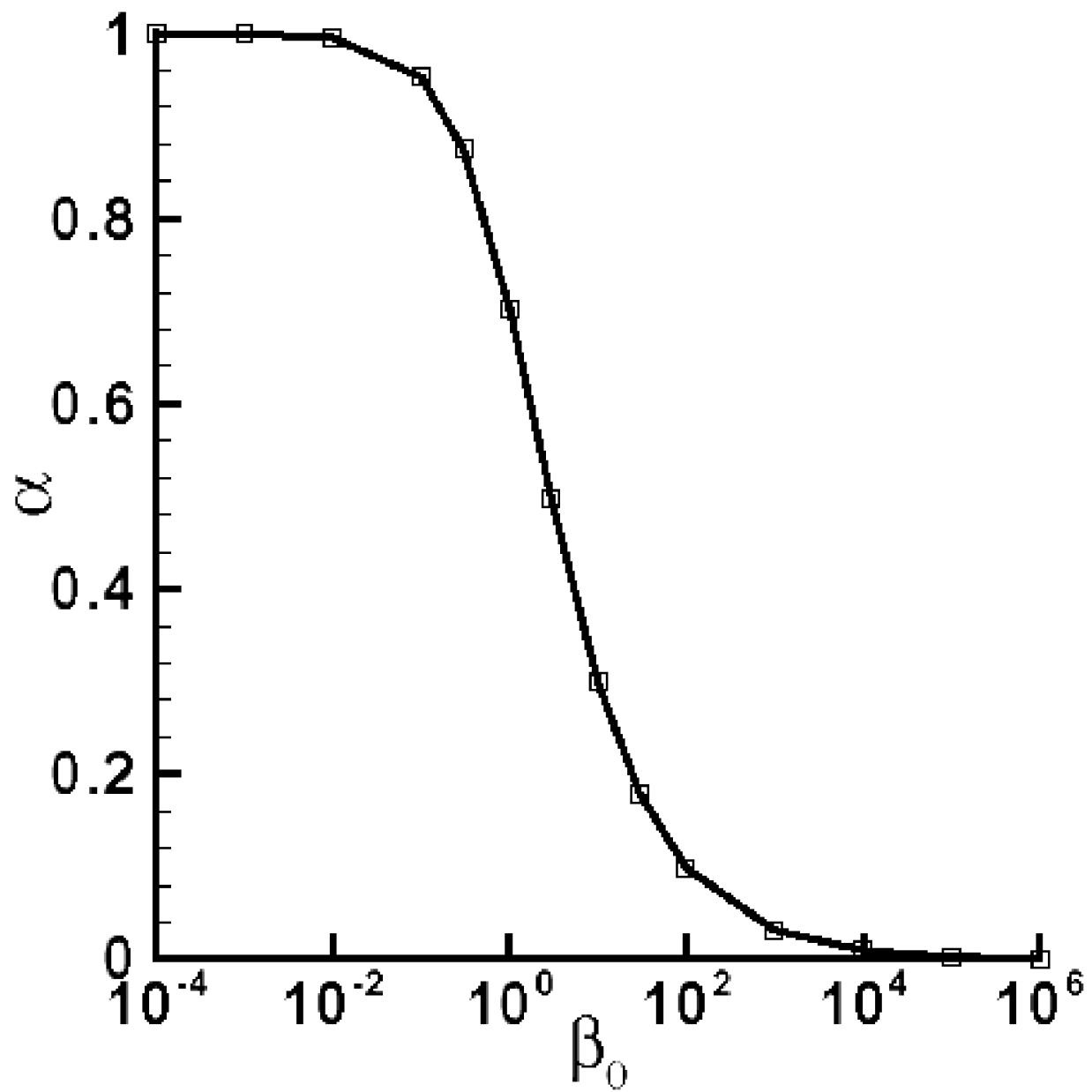


Figure 3: Eigenvalue for point dipole equilibrium (Eq. 2) vs β .

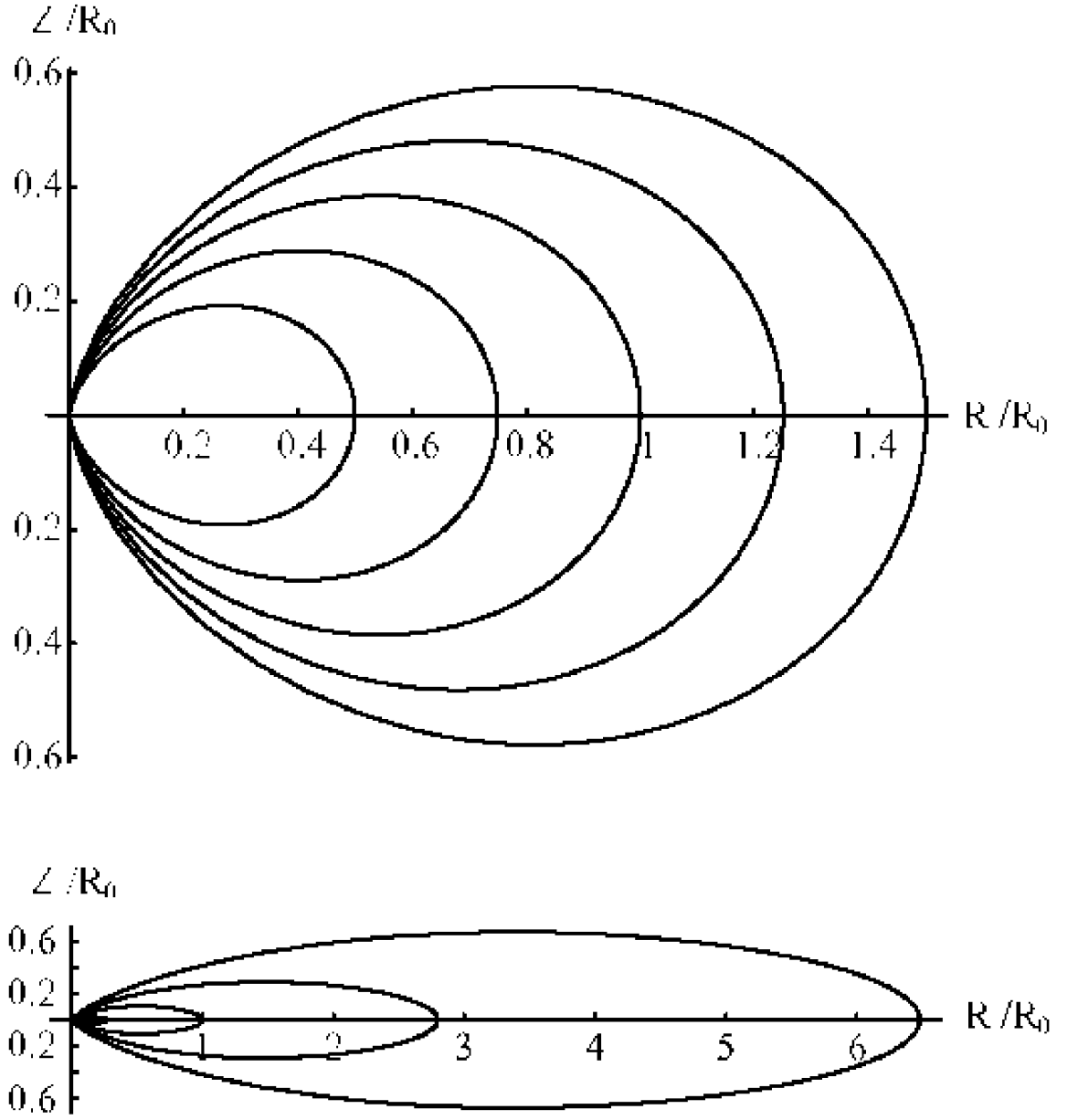


Figure 4: Flux surfaces for point dipole with $\beta=0$ and $\beta=20$.

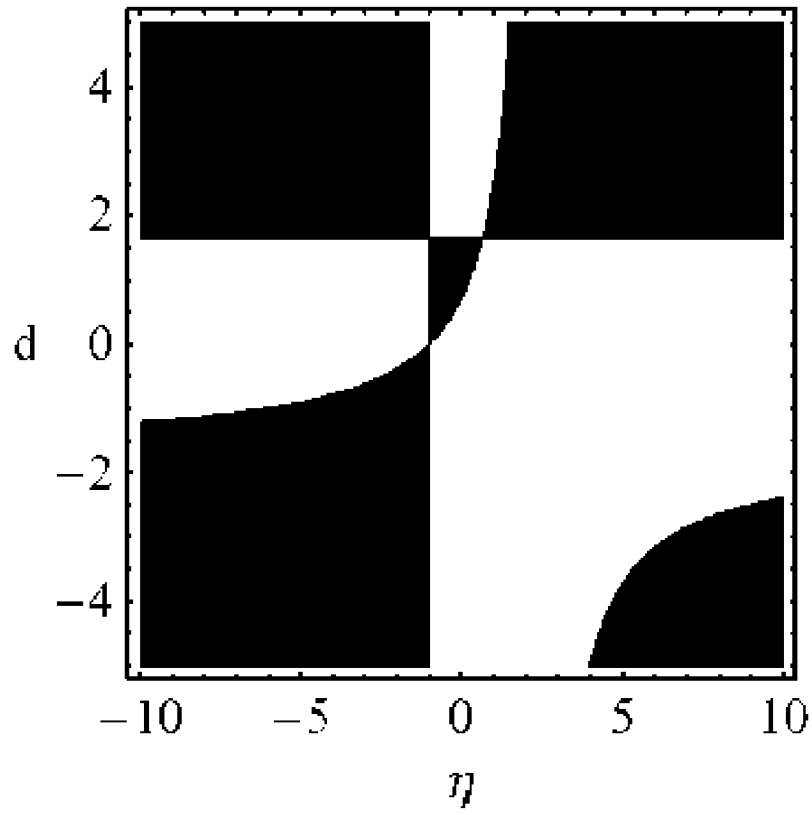


Figure 5: Drift-temperature gradient (DTG) mode stability regions in d - η space. Stability and instability regions are shown in white and grey respectively